

Available online at www.sciencedirect.com

SCIENCE @ DIRECT®

Biochimica et Biophysica Acta 1657 (2004) 61–70

www.bba-direct.com

A study of molecular interactions in light-harvesting complexes LHCIb, CP29, CP26 and CP24 by Stark effect spectroscopy

Dorota Olszówka^a, Stanisław Krawczyk^{a,*}, Waldemar Maksymiec^b

^a*Institute of Physics, Maria Curie-Skłodowska University, P1. M. Curie-Skłodowskiej 1, 20-031 Lublin, Poland*

^b*Institute of Biology, Maria Curie-Skłodowska University, 20-031 Lublin, Poland*

Received 25 June 2003; received in revised form 30 March 2004; accepted 6 April 2004

Available online 28 April 2004

Abstract

Electric field-induced absorption changes (electrochromism or Stark effect) of the light-harvesting PSII pigment–protein complexes LHCIb, CP29, CP26 and CP24 were investigated. The results indicate the lack of strong intermolecular interactions in the chlorophyll *a* (Chl *a*) pools of all complexes. Characteristic features occur in the electronic spectrum of Chl *b*, which reflect the increased values of dipole moment and polarizability differences between the ground and excited states of interacting pigment systems. The strong Stark signal recorded for LHCIb at 650–655 nm is much weaker in CP29, where it is replaced by a unique Stark band at 639 nm. Electrochromism of Chl *b* in CP26 and CP24 is significantly weaker but increased electrochromic parameters were also noticed for the Chl *b* transition at 650 nm. The spectra in the blue region are dominated by xanthophylls. The differences in Stark spectra of Chl *b* are linked to differences in pigment content and organization in individual complexes and point to the possibility of electron exchange interactions between energetically similar and closely spaced Chl *b* molecules.

© 2004 Elsevier B.V. All rights reserved.

Keywords: Light-harvesting; Pigment–protein; Chlorophyll; Photosystem II; Stark spectroscopy; Exciton coupling

1. Introduction

The energy needed by the photosynthetic apparatus of higher plants and algae is provided by pigments arranged into a light-harvesting antenna system. In photosystem II, the antenna pigment–protein complexes surrounding the reaction center comprise the most abundant peripheral trimeric complex LHCIb and three types of minor pigment–proteins: CP29, CP26 and CP24. The monomeric units of all these proteins are products of the same gene family and are all highly similar to the monomeric components of the best known trimeric complex, LHCIb, for which the approximate atomic structure is known [1], but differ in the content of chlorophyll (Chl) *a* and *b* and xanthophyll species. All pigments contained in these complexes function as a very efficient antenna system, and the xanthophylls play an additional and very important role of photoprotectors by quenching the highly reactive electron-

ically excited oxygen, the triplet states generated by chlorophylls, and the excess singlet excited states of chlorophyll under saturating illumination. This last function is ascribed to the minor complexes (CP29, CP26) and is conformationally regulated by calcium ions [2–4]. Mutational analyses of LHCIb [5,6] and CP29 [7] provided a large body of information on the spatial organization of pigment molecules and their interactions as seen mainly by absorption, linear dichroism and circular dichroism spectroscopies. The structural data provide a basis for understanding and interpretation of experimental data and are used for modeling the directionality of the energy transfer process within separate complexes and pigment–pigment interactions, giving rise to spectral differentiation as seen in absorption, linear and circular dichroism spectra [8–11].

Application of different spectroscopic techniques, together with the information on pigment contents and spatial organization of the pigment molecules accumulated in the last several years, could provide a specific insight into the nature of molecular interactions and indicate the molecules involved. Stark effect spectroscopy of the trimeric LHCIb complex demonstrated a strongly en-

* Corresponding author. Tel.: +48-81-376-253; fax: +48-81-537-6191.

E-mail address: SKRAW@TYTAN.UMCS.LUBLIN.PL (S. Krawczyk).

hanced sensitivity to the external electric field of Chls *b* absorbing at 650–655 nm and of a xanthophyll with the (0–0) band at 510 nm, while no large changes were noted in the properties of Chl *a* molecules [12,13]. Generally similar Stark spectra, albeit with slightly shifted transition of the most field-sensitive Chl *b*, were described recently by other authors for LHCIIB monomers, trimers and aggregates [14]. In the present study, we compare the electrochromic properties of pigments in the four antenna complexes of higher plants, and try to correlate some of their spectral features with the spatial organization of pigment molecules and with pigment–pigment interactions.

2. Materials and methods

The antenna complexes LHCIIB, CP29, CP26 and CP24 were separated from PSII particles prepared by the method of Berthold et al. [15], as modified by Dunahay et al. [16]. Protease inhibitors 1 mM benzamidine, 0.2 mM PMSF and 5 mM aminocaproic acid were added to all buffers. To separate the LHCIIB components, the isoelectric focusing technique slightly modified from that described by Dainese et al. [17] was used. The PSII particles containing 5 mg Chl/ml were resuspended in 2 mM EDTA (pH 7.5) in a 4:1 (v/v) ratio. The samples were centrifuged at $40,000 \times g$ for 35 min and then dissociated with 1% dodecylmaltoside (DM) in distilled water on ice. After 30 min, the complexes were separated on the prefocused gel containing 5% Ultradex, 2% Ampholine carrier ampholites (pH 3.5–5.0), 0.06% DM and 1% glycine. The focusing procedure was carried out for 16 h on a 21×7.5 -cm tray. The samples were finally purified and concentrated using the membranes UFC4ODV 25 and YM-3 (Amicon), respectively, and suspended in a solution containing 25 mM HEPES (pH 7.6), 0.06% DM and protease inhibitors.

The samples used in experiments were prepared by mixing the protein suspension with glycerol in 1:2 (v/v) proportion. Samples of CP26 and CP24 were also prepared by adding the protein suspension to 10% solution of polyvinyl alcohol (PVA) in buffer and drying for 5 h at 16–18 °C to obtain a thin (≈ 0.05 mm) transparent foil. This method provided more reliable samples for long-term freezing during the experiments. The maximum absorbance in the Q_y bands of chlorophylls ranged from 0.08 to 0.5. The spectra were recorded using samples in thin (0.06–0.25 mm) cuvettes with transparent glass electrodes coated with an electrically conducting indium-tin oxide layer. The PVA foil was clamped between the electrodes after wetting it with glycerol/water mixture. The absorption and electric field-induced absorbance changes (i.e. Stark effect) spectra were recorded as described in detail previously [18,19]. The values of electrooptical parameters: $\Delta\vec{\mu}$, the excited-minus ground-state difference in permanent dipole moment, and $\Delta\alpha$, the difference polarizability, can be calculated from the

coefficients a_1 and a_2 of the least squares fit approximating the Stark spectrum ($\Delta A(v)$) with the linear combination of the first and second derivatives of the absorption spectrum:

$$\Delta A = a_1 \cdot v \frac{d(A/v)}{dv} + a_2 \cdot v \frac{d^2(A/v)}{dv^2} \quad (1)$$

where:

$$a_1 = \frac{(fF)^2}{15hc} \left\{ \frac{5}{2} \text{Tr}(\Delta\alpha) + (3\cos^2\chi - 1) \times \left(\frac{3}{2} \vec{p} \cdot \Delta\alpha \cdot \vec{p} - \frac{1}{2} \text{Tr}(\Delta\alpha) \right) \right\}, \quad (2)$$

$$a_2 = \frac{(fF)^2}{30h^2c^2} \left\{ |\Delta\vec{\mu}|^2 \cdot [5 + (3\cos^2\chi - 1)] \times (3\cos^2\delta - 1) \right\}, \quad (3)$$

In these formulas [20,21], χ is the angle between the electric vector of light and the vector of applied electric field F and \vec{p} is a unit vector in the direction of the dipole transition moment. Since the experimental data are insufficient to fully determine the difference polarizability tensor $\Delta\alpha$, we calculated the value of $\text{Tr}(\Delta\alpha)$ from spectra recorded at $\chi = 54.7^\circ$. The values of $\Delta\mu$ and $\text{Tr}(\Delta\alpha)$ reported here include the local field factor f which relates the macroscopic (mean) electric field intensity F to the one actually felt by the pigment molecule, i.e. their values represent $f^2 \cdot \text{Tr}(\Delta\alpha)$ and $f \cdot \Delta\mu$.

3. Results

The absorption and Stark spectra in the red spectral range are shown in Fig. 1. The absorption spectra are similar to those published in the literature. The spectra for LHCIIB prepared here with IEF are similar to those obtained previously with samples prepared by electrophoresis on polyacrylamide gel [12] or by the precipitation procedure [12,13]. As can be seen in Fig. 1, the red (Q_y) parts of the Stark spectra are specific to each complex, but the noticeable differences can be divided into three ranges: one covering the absorption bands of Chl *a* (14400–15150 cm^{-1}), and two for Chl *b* (15150–15500 and 15500–16000 cm^{-1}). The Stark spectra in the region of Chl *a* bands are roughly similar in shape and intensity as indicated also by the electrooptical parameters of Chl *a* (see below) for all three minor complexes. However, a large variability is seen in the spectral region of Chl *b* comprising the biphasic Stark bands centered at 15240 cm^{-1} (656 nm) with the maximum and minimum at 15170 and 15300 cm^{-1} in LHCIIB, at 15300 cm^{-1} (with the positive and negative extrema at 15230 and 15380 cm^{-1} , respectively) in all minor complexes, and the one centered at 15640 cm^{-1} with strong features at 15570(+) and 15700(–)

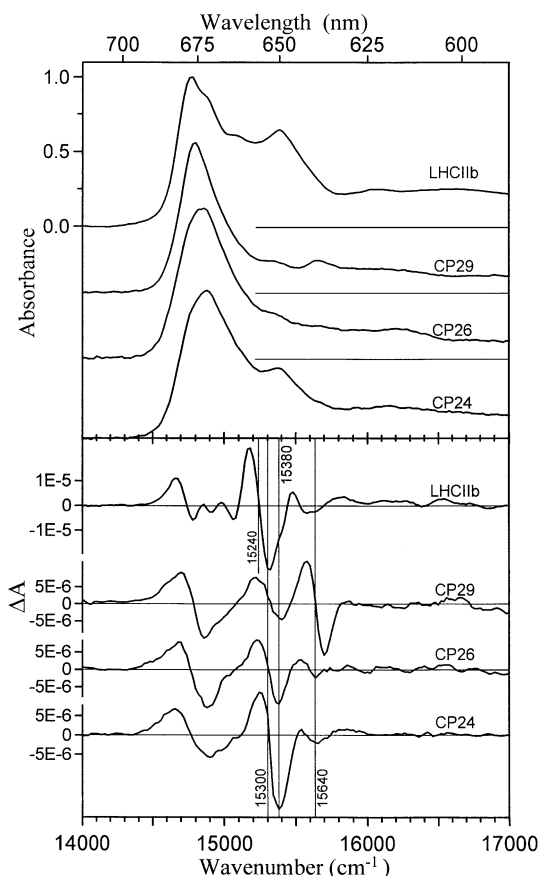


Fig. 1. Absorption (upper part) and Stark spectra (lower part) of the antenna pigment–proteins in the region of the Q_y absorption bands of chlorophylls. The spectra of LHCIIb, CP29 and CP26 were recorded in 66% glycerol with aqueous buffer and for CP24 in polyvinyl alcohol film. The spectra have been scaled to maximum absorbance of 1.0 and the Stark spectra additionally to the electric field intensity 1×10^5 V/cm. Temperatures: 110–130 K.

cm^{-1} in CP29. The values of $\Delta\mu$ and $\text{Tr}(\Delta\alpha)$ obtained from fits performed according to Eq. (1) in these three spectral ranges are quoted in Table 1.

3.1. Chlorophyll *a*

For LHCIIb, both the quality of the fit (not shown) and the mean values of electrooptical parameters for the spectral forms of Chl *a* in the range $14500\text{--}15050\text{ cm}^{-1}$, determined with the derivatives of absorption according to Eq.

(1), $\Delta\mu \cong 0.8\text{--}1\text{ D}$, $\text{Tr}(\Delta\alpha) = 20\text{--}35\text{ \AA}^3$, were similar to those obtained in the previous study for Chl *a* in LHCIIb [12] and to the values for Q_y transition in monomeric Chl *a*: $\Delta\mu = (0.9 \pm 0.1)\text{D}$, $\text{Tr}(\Delta\alpha) = (18 \pm 4)\text{ \AA}^3$

(the values of $\Delta\alpha$ from our previous work [12] should be multiplied by 3 to convert them into $\text{Tr}(\Delta\alpha)$ used here).

Figs. 2–4 present fits of Stark spectra based on absorption derivatives according to Eq. (1), which were obtained separately for each of the spectral ranges of Chl *a* and Chl *b* specified above. The values of $\Delta\mu$ and $\text{Tr}(\Delta\alpha)$ are quoted in Table 1. In the range comprising essentially all Chls *a* ($14400\text{--}15150\text{ cm}^{-1}$), the parameters estimated are considered to represent the mean values of $\Delta\mu$ and $\Delta\alpha$ for this pigment pool. Although these mean values are not very different from those for monomeric Chl *a*, the fits in the range of Chl *a* Q_y bands for CP29 and CP26 indicate the occurrence of noticeable differences between individual electronic transitions which do not conform to a common set of electrooptical parameters. Only the Stark spectrum of CP24 indicates more homogeneity in the electrooptical parameters of Chls *a*, which makes this complex more similar to LHCIIb in this regard.

3.2. Chlorophyll *b*

There are remarkable differences between the Stark spectra of all complexes examined in the spectral range covering the absorption bands of Chl *b* (cf. Fig. 1). Our work on LHCIIb [12,13] revealed a complex structure of the biphasic Stark band centered at 15240 cm^{-1} ($15170/15300\text{ cm}^{-1}$, Fig. 1). In the Stark spectrum of LHCIIb the strong biphasic Stark band centered at 15240 cm^{-1} and ascribable to Chl *b* is associated with a large polarizability change, $\text{Tr}(\Delta\alpha) \approx 280\text{ \AA}^3$, and $\Delta\mu = 1.9\text{--}2.7\text{ D}$ [12], which are to be compared with the data for Chl *b* monomer:

$$\Delta\mu = (1.3 \pm 0.3)\text{D}, \text{Tr}(\Delta\alpha) = 70\text{ \AA}^3$$

(unpublished data). No new estimates were tried in the present study for this transition and for the other minor transitions in LHCIIb.

Our work on LHCIIb [12,13] revealed a complex structure of the biphasic Stark band centered at 15240 cm^{-1} ($15170/15300\text{ cm}^{-1}$, Fig. 1). In addition to the dominating biphasic component, there is another weaker transition

Table 1

Mean values of electrooptical parameters (dipole moment change, $\Delta\mu$, and polarizability change, $\text{Tr}(\Delta\alpha)$) on electronic excitation for the Chl Q_y transitions in the three spectral ranges corresponding to Chl *a* and to the two distinct features in Chl *b* spectra obtained from fits of Stark spectra with the linear combination of absorption derivatives

Spectral range (cm^{-1})	LHCIIb		CP29		CP26		CP24	
	$\Delta\mu$ (D)	$\text{Tr}(\Delta\alpha)$ (\AA^3)	$\Delta\mu$ (D)	$\text{Tr}(\Delta\alpha)$ (\AA^3)	$\Delta\mu$ (D)	$\text{Tr}(\Delta\alpha)$ (\AA^3)	$\Delta\mu$ (D)	$\text{Tr}(\Delta\alpha)$ (\AA^3)
14000–15150 (Chl <i>a</i>)	0.8–1	20–35	0.5	35	0.9–1	25–35	0.8–1	20–25
15150–15500 (Chl <i>b</i>)	1.9–2.7	200	2.2–2.6	80–130	2.9–3.3	170–220	2.5–3	80–110
15500–16000 (Chl <i>b</i>)	1–2	–	1.7–2.1	420–570	–	–	–	–

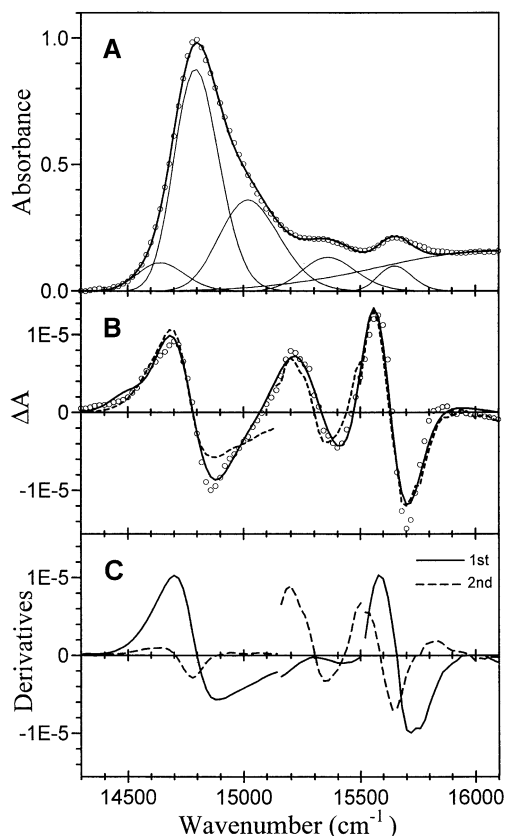


Fig. 2. (A) Absorption spectrum; (B) Stark spectrum of CP29. Points are experimental data, continuous lines are the results of simultaneous fits to both spectra with log-normal components, and the dashed lines in B are the local fits whose first- and second-derivative components are shown in panel (C) CP29 in 66% glycerol/aqueous buffer, temperature: 130 K. Spectra were scaled to unit absorbance and to $F=10^5$ V/cm.

indicated by an inflexion at 15400 cm^{-1} , which becomes more significant after partial photooxidation of Chl *b* [13]. These details of spectral structure were observed in all our data for LHCIIb prepared using polyacrylamide gel electrophoresis, cation precipitation or isoelectric focusing techniques. In a recent paper [14], the minimum of the Stark band was found at 650 nm (15380 cm^{-1}), which seems to correspond to the higher-energy component in our spectra. Although the explanation of this difference cannot be given immediately, we would like to indicate that the mechanism leading to the increased values of $\Delta\mu$ and $\Delta\alpha$ based on weak admixture of charge resonance states (see below) can lead to observable effects in case of even very small structural differences.

The local fits within the range $15150\text{--}15500\text{ cm}^{-1}$ comprising the Chl *b* feature in the Stark spectra of minor complexes are shown in Figs. 2–4. The fits were performed using the derivatives of the absorption spectrum and thus include the bands of some pigment(s) with specific properties reflected by a stronger signal as well as the neighbouring overlapping bands with different electrooptical characteristics. Figs. 2–4 also show the first and second derivative components of the fitting curves. In each case, the

second derivative component dominates and this is reflected by the values of $\Delta\mu \approx 2.2\text{--}3.3\text{ D}$, which are remarkably larger than for monomeric Chl *b*. Also the values of $\text{Tr}(\Delta\alpha)$, although associated with a weaker fit component, are increased in comparison with the data for Chl *b* monomer (cf. Table 1).

CP29 is the only complex which presents a strong electrochromism of Chl *b* associated with the highest energy Q_y transition discernible in PSII antenna complexes at 15640 cm^{-1} (639 nm). The comparison of absorption and Stark effect spectra in this region indicates that this spectral feature has clearly the first-derivative shape, which reflects the prevailing contribution of polarizability to the energy change of corresponding electronic transition in the electric field. Indeed, it is characterized with an increased value of $\Delta\mu \approx 2\text{ D}$ and a large polarizability change on electronic excitation, $\text{Tr}(\Delta\alpha) \approx 420\text{--}570\text{ \AA}^3$ (cf. Table 1). In the Stark spectrum of LHCIIb, there is a shallow double minimum at this position originating from two transitions on the slope of Chl *b* band between 15500 and 15700 cm^{-1} [12,13]. Similar weak negative bands occur in Stark spectra of CP26 and CP24. Since the minima in Stark spectra of CP26 and CP24 approximately coincide with these weak absorption bands at 15640 cm^{-1} , it can be inferred that their electrochromism is not dominated by the first-deriva-

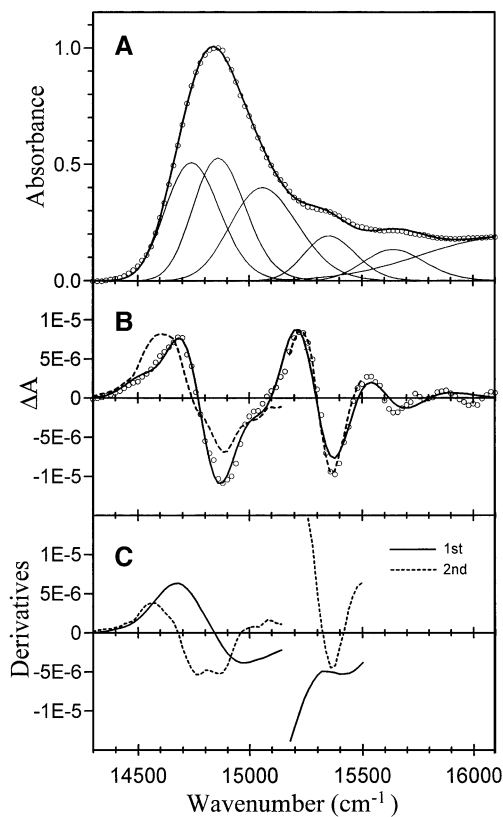


Fig. 3. (A) Absorption spectrum of CP26; (B) Stark spectrum; (C) components of local fits shown in panel B. CP26 in 70% glycerol/aqueous buffer, temperature: 110 K. Other details as in Fig. 2.

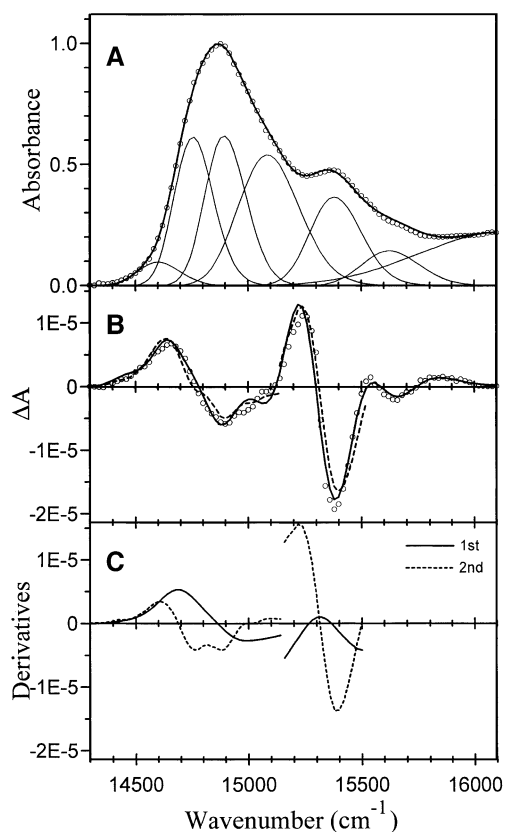


Fig. 4. (A) Absorption spectrum of CP24; (B) Stark spectrum; (C) components of local fits shown in panel B. CP24 in PVA film, temperature: 130 K. Other details as in Fig. 2.

tive component. However, due to the weakness of these features, no estimates for $\Delta\mu$ and $\Delta\alpha$ were attempted.

3.3. Deconvolution of Q_y bands

As mentioned above, the deficiencies in the fits of Stark spectra in the Chl *a* absorption range for CP29 and CP26 indicate that $\Delta\mu$ and $\Delta\alpha$ may be different for some electronic transitions within the Chl *a* pool. Also, the fits to Stark spectra associated with weakly expressed absorption bands, which occur in the region of Chl *b* absorption, potentially can be affected by the spectral overlap. In order to decrease the significance of these unfavorable circumstances, we performed the simultaneous deconvolution of absorption and Stark spectra with sets of log-normal components [22] by minimizing the sum of appropriately weighted squared deviations of the fits from both spectra. The starting positions of the component bands were determined from the minima in the second derivative of the absorption spectrum. We noted a remarkable agreement between the data so obtained and the mean values from Gaussian deconvolution of normal- and low-temperature absorption spectra in Ref. [23] as to the band positions, in most cases within less than 30 cm^{-1} (1.5 nm). Band positions determined in this way were allowed to change by not more than 30 cm^{-1} in the

fitting procedure. The results are presented in Figs. 2–4 and the electrooptical parameters estimated for each of the component bands are quoted in Table 2. The values of $\Delta\mu$ and $\text{Tr}(\Delta\alpha)$ obtained from spectral deconvolution are generally similar to the values resulting from direct fits (cf. Table 1). The differences stem partly from a slightly larger curvature of the fits to the absorption spectra which, being guided only by the clearly distinguishable features in the spectra, pass over a number of weaker components. Both methods of parameter estimation suffer from their specific deficiencies and, considering the exact numerical values of the parameters obtained, one must take into account their possible errors, which for $\text{Tr}(\Delta\alpha)$ can reach 25–30% and about 15% for $\Delta\mu$. Despite the differences between $\Delta\mu$ and $\text{Tr}(\Delta\alpha)$ for individual transitions among Chls *a*, their values remain not very different from those for Chl *a* monomers. The main conclusion from both types of fits is that the electrooptical parameters for Chl *b* transitions at 15640 cm^{-1} (639 nm) in CP29 and at 15380 cm^{-1} (650 nm) in CP26 and possibly also in CP24 are remarkably enhanced as compared to the values for monomeric pigments. In the case of CP24, the increase in absorption at 15380 cm^{-1} due to the presence of an additional Chl *b* with “monomeric” properties may have a masking effect on enhanced electrochromism of other Chls *b*.

3.4. Xanthophyll and Soret bands

Absorption and Stark spectra in the blue region shown in Fig. 5 show substantial differences between the spectra of LHCIIB and the three minor complexes. The large absorption of LHCIIB in the range $19000\text{--}22000\text{ cm}^{-1}$ can be attributed to its large Chl *b* content. The strong feature originating from the weak xanthophyll absorption band at 510 nm (19600 cm^{-1}) suggests that the rest of the spectrum contains also a substantial contribution from this xanthophyll. In a recent work [13], we demonstrated this semi-quantitatively by showing that the Stark spectrum of

Table 2

Electrooptical parameters for electronic transitions represented by log-normal components in the simultaneous fits to absorption and Stark effect spectra of the minor light-harvesting complexes

CP29			CP26			CP24		
ν (cm^{-1})	$\Delta\mu$ (D)	Tr ($\Delta\alpha$) (\AA^3)	ν (cm^{-1})	$\Delta\mu$ (D)	Tr ($\Delta\alpha$) (\AA^3)	ν (cm^{-1})	$\Delta\mu$ (D)	Tr ($\Delta\alpha$) (\AA^3)
14640	1	65	14740	1.0	17	14756	0.7	35
14795	0.4	55	14860	1.4	20	14896	0.9	15
15020	0.4	20	15060	1.6	14	15090	1.6	30
15360	1.4	230	15355	2.4	155	15380	2.2	75
15650	1.3	460	–	–	–	–	–	–

The upper three data rows correspond to Chl *a* and the lower two to Chl *b*. The data in each of the triple column contain the position of the band center in cm^{-1} and the corresponding dipole moment and polarizability changes. The asymmetry parameter in log-normal components (a free variable in the fits) was very small, from 0.05 to 0.11, making the curves nearly Gaussian.

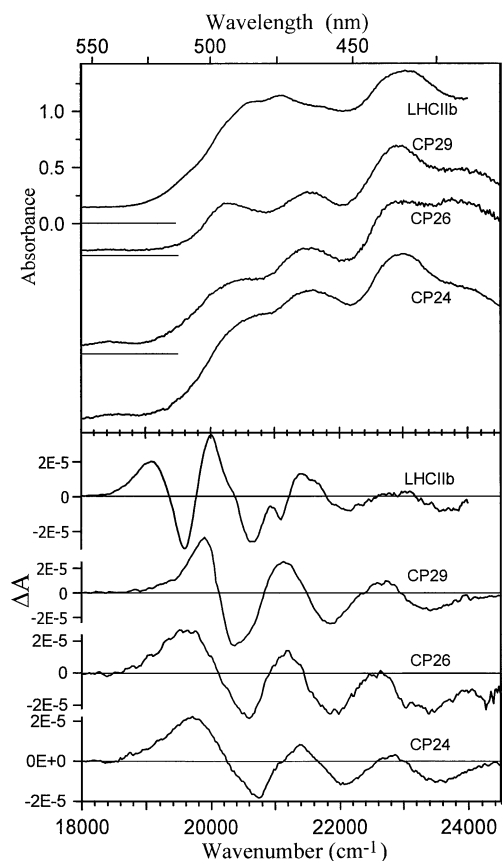


Fig. 5. Absorption (upper part) and Stark spectra (lower part) in the region of xanthophyll and chlorophyll Soret bands. Experimental details as in Fig. 1.

LHCIIb can be reconstructed from three xanthophyll components appropriately shifted to mimic the contributions from Xan510, Lut and Neo, with the electrooptical parameters of the latter two components close to those for xanthophylls in vitro.

The coincidence of the minimum in the Stark spectrum of LHCIIb at 19600 cm^{-1} with a minimum in the second derivative of absorption (not shown here) allowed for an approximate estimate of the dipole moment change, $\Delta\mu \geq 10\text{ D}$ [12], associated with the electronic transition in a xanthophyll absorbing in this region (510 nm). Fig. 6 presents an example of simultaneous deconvolution of absorption and Stark spectra for LHCIIb. The result significantly depends on the arbitrarily chosen spectral range fitted and on the assumed preferences for better approximating either the absorption or the Stark spectrum. Although the parameters of the higher-energy components of the fit are not unique, the lowest-energy component corresponding to the transition at 19600 cm^{-1} is reasonably stable, being strongly conditioned on its half-width which is closely related to the zero-crossing points in the Stark spectrum. The values of $\Delta\mu$ obtained in this way fall in the range 9–12 D with negligible contribution from $\Delta\alpha$. Gaussian deconvolution of similar Stark and

absorption spectra in a recent work by other authors [14] has led to an estimate of $\Delta\mu = (14.6 \pm 2)\text{ D}$ for this xanthophyll.

The Stark spectra of the minor complexes in the region up to 22000 cm^{-1} , particularly of CP29 which has the lowest Chl *b/a* ratio [24], can be considered to originate mainly from xanthophylls which generate much stronger Stark signals than chlorophylls. In the Stark spectrum of CP29, the negative band in the range $20200\text{--}20800\text{ cm}^{-1}$ is asymmetric and exhibits the presence of a shoulder at $20600\text{--}20700\text{ cm}^{-1}$. This feature is attributable to the negative band of Neo which absorbs at 20530 cm^{-1} (487 nm) in LHCIIb [25], and thus its negative Stark signal can be expected at about 100 cm^{-1} to the blue. Indeed, the band at 20250 cm^{-1} splits into two overlapping components in the absorption spectrum of CP29 at very low temperature (5 K) [26] with the higher energy component attributable to Neo.

In the minor complexes, the site L2 is considered to bind Lut, Neo or Vio [7,27,28]. Native complexes were shown to contain these xanthophylls in different proportions, with the highest content of Neo in LHCIIb and its lack in CP24, and an inverse trend for Vio, which is the only xanthophyll besides one Lut in CP24. In line with this trend, the Stark spectra (Fig. 5) exhibit a shift of the minima toward the violet in accordance with the increasing content of Vio, which has the shortest conjugated chain

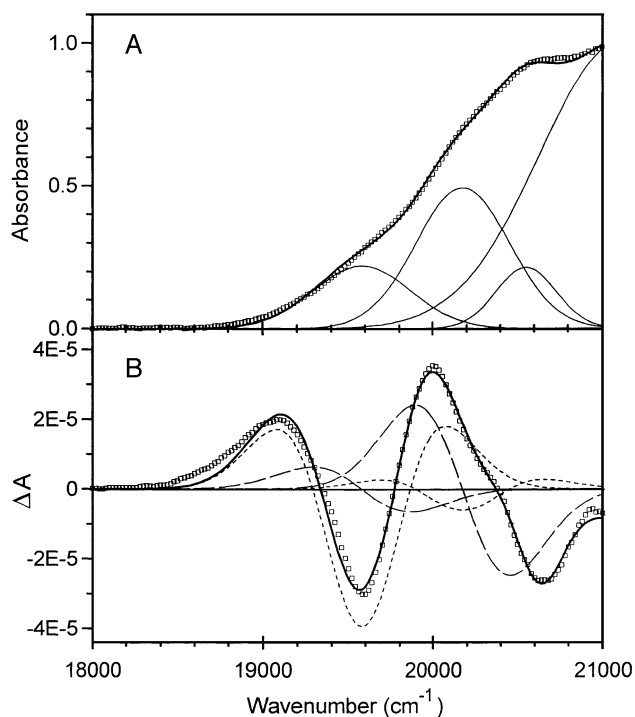


Fig. 6. (A) Absorption and (B) Stark spectrum of LHCIIb with the results of simultaneous fit of both spectra. Points are experimental data, continuous lines are the fitting curves and the first and second derivatives are shown with dashed and dotted lines. A constant background was subtracted from the absorption spectrum.

and the most blue-shifted spectrum. The general similarity of Stark spectra in the violet for CP24 and CP26 (and to a significant degree for CP29) complexes with different Chl *b* contents illustrates the dominance of field-induced absorbance changes originating from xanthophylls over those from chlorophyll. However, we did not succeed in obtaining reliable fits to Stark spectra and estimates for $\Delta\alpha$ and $\Delta\mu$ using the combination of absorption derivatives, because of the spectral overlap and significant contribution to the absorption spectra by Chl *b*.

4. Discussion

4.1. Chlorophyll *a*

The different spectral features exhibited by the antenna complexes described in the preceding section stem from differences in pigment contents and from spatial configuration of pigment molecules that determine their interactions. Previous studies of the Stark effect in LHCIIB, both ours [12] and by other authors [14], indicated the lack of strong interactions within the Chl *a* pool and a significant modification of the electronic structure of some Chls *b* absorbing at 15200–15400 cm⁻¹ (652–656 nm) and the xanthophyll absorbing at 19600 cm⁻¹ (510 nm). The results of the present work indicate the lack of interactions that could significantly modify the electronic structure of Chl *a* also in the three minor antenna complexes of PSII, as indicated by the electrooptical parameters for their Chl *a* pools quoted in Tables 1 and 2. The values of $\Delta\mu$ and $\text{Tr}(\Delta\alpha)$ not exceeding those for Q_y transition in monomeric Chl *a* are characteristic for purely coulombic interactions not involving the electron exchange effects [12,29]. Some inhomogeneity among Chl *a* transitions indicates that the coupling of electronic transitions of Chls *a* can lead to observable differences between individual transitions in Stark spectra, but more detailed analysis of these effects could be performed only at better spectral resolution, probably attainable at much lower temperatures.

4.2. Chlorophyll *b* in LHCIIB and CP29

The differences between Stark bands of Chl *b* in individual complexes may reflect different occupation of binding sites, as revealed in mutational studies of monomeric LHCIIB subunits [5] and of CP29 [7]. These studies introduced corrections to the original assignments of Chl *a* to seven sites, A1–A7, and of Chl *b* to five sites, B1–B6 (except of B4), revealed in the crystallographic structure of LHCIIB [1], by assigning Chl *b* to site A7, Chl *a* to site B1, and allowing for mixed *a/b* occupancy for sites A3, A6 and B3. However, the mixed occupancy was not observed for site B3 in reconstituted LHCIIB trimers [6].

The Chl *b* molecules generating the Stark signals at 15200–15400 cm⁻¹ associated with increased polarizability difference can be those with similar excitation energies and making close contacts. According to the approximate crystallographic structure of LHCIIB [1] and to spectral assignments for mutant proteins [5–7,28], these can be:

- the trimer A6(*b*652/*a*678)·B6(*b*652)·A7(*b*652) with A7–B6 center-to-center and closest approach distances 10 and 4 Å, respectively, and 8.7, 4 Å for the B6–A6 pair, or
- the dimer A3(*b*650/*a*662)·B3(*b*650/*a*665) with distances of 9 and 4 Å.

The distances given above refer to the structure of LHCIIB and the symbols in parentheses denote the absorption wavelength of Chl species. In the above specification, we fully account for the mixed occupancy of some sites. If it were not the case (as claimed for B3 site [6]), the possibilities would reduce to only B6(*b*652)A7(*b*652) interaction in LHCIIB. Under the assumption of similar pigment organization and intermolecular distances in CP29 and LHCIIB, the spectral assignments for CP29 point to only one pair of closely spaced sites, A3(*a*668/*b*638)·B3(*a*679/*b*639), with the pigment content capable of giving rise to the strong electrochromism corresponding to the Chl *b* absorption band at 15640 cm⁻¹ (639 nm), if in the A3(*b*638)·B3(*b*639) configuration. Similar conclusion concerning the interaction of Chls *b* in A3 and B3 sites was reached in a recent study of CP29 on the basis of time-resolved spectroscopic methods [30]. It should be noted that other configurations of these sites allowed by mixed occupancy (e.g. *ab*, *ba* or *aa*) would not result in extensive mixing of excited states because of larger spacing in the transition energies; they can thus not be revealed in Stark spectra. Although these assignments depend on still uncertain details of molecular distances and orientations, it seems that Stark spectra deliver information compatible with the allocation of spectral forms deduced from genetically modified antenna proteins.

4.3. Chlorophyll *b* in CP26 and CP24

The Stark spectrum of CP26 contains the biphasic Chl *b* band at 15200–15400 cm⁻¹ similar to that in CP29, but lacks the strong Stark band centered at 15640 cm⁻¹ and has a lowered absorption at this position. In the study on pigment reconstitution into CP26 [28], it was concluded that the pigment binding properties of CP26 are similar to CP29, except for one additional Chl *b* bound in the B2 site, and absorbing at 648–650 nm (\approx 15400 cm⁻¹). In accordance with this assignment, there is a relative increase in absorbance at 15300–15400 cm⁻¹ in CP26 spectrum compared to that for CP29. The electrooptical parameters for the range 15150–15500 cm⁻¹ in CP29 and CP26 are two to three times larger than for Chl *b* monomer (Table 1) as are also the parameters for the

$\approx 15360 \text{ cm}^{-1}$ bands obtained from deconvolution procedure for these complexes (Table 2). However, the data for CP29 and CP26 do not differ so clearly as to indicate the involvement of the additional Chl *b* in CP26 into strong interactions changing its electronic properties.

In the Stark spectra of CP24, the band related to the Chl *b* absorption at 15380 cm^{-1} (650 nm) contains mainly the second derivative signal (Fig. 4C) and, in both types of fits, it is associated with an increase in $\Delta\mu$. In comparison with CP26, CP24 contains about one additional Chl *b* at unknown binding site [27], and an additional complication may arise from the lack of helix D which can affect binding capability of site B3. If pigment allocation in CP26 is that in CP29 [7] supplemented with one Chl *b* in site B2, then of the 12 Chl binding sites occupied in LHCIIB, three sites remain available for the additional Chl: A6, A7 and B1. Sites A7 and B1 bind only Chl *b* and A6 is a mixed site in LHCIIB [5]. It is not known which site binds the tenth Chl (*b*) [28]. Extending the observations from LHCIIB, we can conclude that binding this Chl *b* in either A6 or A7 can lead to its strong interactions with Chl *b* in site B6 placed between them. Since the data for this Chl *b* band of CP24 in Tables 1 and 2 do not indicate a large increase of $\Delta\mu$ or $\text{Tr}(\Delta\alpha)$, a distant B1 localization can be inferred for this Chl *b* as well.

4.4. Xanthophylls

Since the Stark spectra of Lut495 and Neo in LHCIIB originate from essentially unperturbed pigments [13], their minima should be located about 100 cm^{-1} to the blue from the corresponding absorption maxima. Thus, the coincidence of the negative band at 20300 cm^{-1} in CP29 spectrum with a weak sign of a negative band at the same position in LHCIIB on the positive lobe due to Xan510 [13] can be attributed to the same Lut495 in the L1 site present in both complexes, in accordance with other assignments concerning this site.

The nature of the xanthophyll in LHCIIB with absorption spectrum starting at 510 nm has been a subject of different assignments. It was considered to be a violaxanthin bound at an unknown site [31,32]; consistently with this, the two lutein molecules were indicated to absorb with their (0–0) bands at 495 nm (20200 cm^{-1}), or with one of them at 489 nm (20450 cm^{-1}) [33,34]. Recent assignments based on resonance Raman investigations [35,36], triplet-minus-singlet spectra [37] and Stark spectroscopy [14] have shown that the xanthophyll absorbing at 510 nm is a lutein molecule bound in site L2. An important observation supporting this assignment is that the dissociation of LHCIIB trimers into monomers causes the disappearance of the 510-nm band from both absorption and Stark spectra and a significant gain of the Stark band of lutein at $491\text{--}3 \text{ nm}$ (20300 cm^{-1}) [14].

The deconvolution of Stark spectra opens a possibility to estimate the quantity of Xan510 present in the monomer

of LHCIIB from the dipole strength of Xan510 spectrum which starts at 19600 cm^{-1} with the (0–0) band. To determine the latter, the entire absorption spectrum of LHCIIB was divided by the wave number and scaled so as to make the integral

$$\int \frac{\varepsilon(\nu)}{\nu} d\nu \quad (4)$$

over the range of Q_y transitions to correspond to the total dipole strength of Chls *a* and *b*. This was performed by taking the dipole transition moments as 4.38 D for Chl *a* and 3.64 D for Chl *b* [8,10,11,38] and assuming that the integral (Eq. (4)) in the spectral range from 14200 cm^{-1} to 15800 cm^{-1} should correspond to the dipole strength of seven Chls *a* and five Chls *b*. Then, the dipole strength of the (0–0) band of Xan510 was calculated using the scaled absorption spectrum. From a separate analysis of absorption spectra of violaxanthin, lutein and lycopene, we obtained the ratio of the integral (Eq. (4)) for the (0–0) transition to that for the entire absorption spectrum of the carotenoid as equal to 0.28 ± 0.02 . Using this ratio, we obtain the dipole strength for Xan510 as equal to 120 D^2 . Since LHCIIB may contain up to eight Chls *a* and six Chls *b* [39], the other estimate can be equal to 140 D^2 . Compared with the dipole strength for lutein which we determined to be 182 D^2 , this means about 0.66–0.77 molecules of Xan510 per LHCIIB monomer (even a larger number if it is considered to be violaxanthin with a smaller dipole strength of 162 D^2). Although these values bear different errors with the biggest one related to the fitting procedure, which can approach about 20%, they certainly indicate a larger number of molecules involved than the number of $\approx 0.2\text{--}0.3$ violaxanthin molecules known to occur per LHCIIB monomer [5,34], thus pointing to the assignment of Xan510 to lutein.

According to the studies on LHCIIB mutant lacking Neo [25,34], the binding of Neo in LHCIIB affects the absorption properties of a Chl *b* molecule located near this xanthophyll site and absorbing at 651 and 465 nm. The Neo binding site is localized close to the helix C and to the group of Chls *b* in sites A6, B6 and A7. The Stark spectra of LHCIIB [13] indicated the lack of significant perturbation of the electronic states in Neo, thus suggesting an indirect influence of Neo on the Chl-Chl coupling through a structural modification of the protein. The possible role of electron exchange interactions between Chls *b* suggested above offers a plausible explanation for the spectral effects of Neo binding. The involvement of short-range exchange interactions between Chls *b* bound in the sites A6, B6, A7 and absorbing around 650 nm could be a factor particularly sensitive to a structural perturbation. Therefore, even a small structural modification changing the closest interatomic distances induced by binding of Neo can exert large influence on charge resonance states in the Chl *b* ensemble and thus lead to the hypochromicity at 465 nm and a hyperchromicity as

well as smaller effects of band shifts observed around 651 nm [25,34].

5. Final remarks

Stark spectra of the minor antenna complexes of PSII indicate the lack of significant modification of the electronic structure of Chl *a* molecules, which makes these complexes similar to LHCIIb in this respect. This is not the case for Chl *b*. The strongest electrochromism detected for CP29 is associated with the electronic transition at $15\,640\text{ cm}^{-1}$ (639 nm). This feature makes it similar to the $\approx 655\text{-nm}$ band of Chl *b* in LHCIIb detected previously and confirmed in this work. These electronic transitions in LHCIIb and CP29 are accompanied by a substantial increase in polarizability and dipole moment changes on excitation. In both cases, the effects observed can be related to pigments whose closely lying sites of binding allow to postulate the involvement of charge resonance states. As we have already indicated [12] and confirmed for the case of acridine orange dimer [29], exciton coupling limited to the transition moment interactions is insufficient to explain the remarkably increased values of difference dipole moments and polarizabilities. Similar but less well expressed features seem to be associated with Chl *b* transitions at $15\,300\text{--}15\,400\text{ cm}^{-1}$ (649–653 nm) in CP26 and CP24, but may be partly masked by spectral overlap. Such a conclusion is supported by observations for systems where the known molecular structure indicates exciton coupling and the possibility of close molecular contacts. These are the cases of bacterial antenna LH1 [40,41] and LH2 [40–42] which exhibit polarizability changes of 1300–1800 and 600–1400 \AA^3 , respectively, compared with negligibly small $\Delta\alpha$ for monomeric bacteriochlorophyll, Photosystem I antenna [43] ($\Delta\alpha \approx 300\text{ \AA}^3$ for some Chls *a*), and of bacterial reaction centers where the large dipole moment change reflects a large polarizability increase of the special pair dimer in a permanent electric field of the protein environment [44].

The lutein molecule in LHCIIb absorbing at 510 nm exhibits a large difference dipole and the absorption spectrum shifted by 600 cm^{-1} from about 495 nm. If assumed to be due to the electric field of the protein, the difference dipole induced in lutein with uniaxial polarizability of $\Delta\alpha \approx 1000\text{ \AA}^3$ [19] means the electric field intensity of 3–4.5 MV/cm, which according to the relation $hc\cdot\Delta\nu = \Delta\alpha\cdot F^2/2$, implies a spectral shift $\Delta\nu$ in the range $250\text{--}560\text{ cm}^{-1}$. This result is reasonably close to the estimated spectral shift of 600 cm^{-1} . In the case of a point charge as a source of the field, calculations [45] predict a significant variability of the shift in excitation energy, which, depending on the position of the charge relative to the conjugated chain, can significantly exceed the value estimated above for a homogeneous electric field.

Note added in proof

After submission of this paper a new crystallographic structure of LHCIIb appeared (Z. Liu et al., Nature 428 (2004) 287–292) which confirms the assignment of chlorophylls *b* to the sites B6 and A7 (now referred to as Chl *b* 606 and 607) and points to their close spacing with the shortest interatomic distance of 3.67 Angstrom (according to data in Supplementary Information).

Acknowledgements

This work was supported by research funds of the Maria Curie-Skłodowska University and by grant no. 3P04A 05723 from the State Committee for Scientific Research.

References

- [1] W. Kuhlbrandt, D.N. Wang, Y. Fujiyoshi, Atomic model of plant light-harvesting complex by electron crystallography, Nature 367 (1994) 614–621.
- [2] R.J. Debus, A.P. Nguyen, A.B. Conway, H.-A. Chu, Identification of manganese or calcium ligands in Photosystem II by site-directed mutagenesis, Biophys. J. 59 (1991) 143a.
- [3] P. Pesaresi, D. Sandona, E. Giuffra, R. Bassi, A single point mutation (E166Q) prevents dicyclohexylcarbodiimide binding to the photosystem II subunit CP29, FEBS Lett. 402 (1997) 151–156.
- [4] C. Jegerschold, A.W. Rutherford, T.A. Mattioli, M. Crimi, R. Bassi, Calcium binding to the photosystem II subunit CP29, J. Biol. Chem. 275 (2000) 12781–12788.
- [5] R. Remelli, C. Varotto, D. Sandona, R. Croce, R. Bassi, Chlorophyll binding to monomeric light-harvesting complex, J. Biol. Chem. 274 (1999) 33510–33521.
- [6] H. Rogl, R. Schodel, H. Lokstein, W. Kuhlbrandt, A. Schubert, Assignment of spectral substructures to pigment-binding sites in higher plant light-harvesting complex LHCI, Biochemistry 41 (2002) 2281–2287.
- [7] R. Bassi, R. Croce, D. Cugini, D. Sandona, Mutational analysis of a higher plant antenna protein provides identification of chromophores bound into multiple sites, Proc. Natl. Acad. Sci. U. S. A. 96 (1999) 10056–10061.
- [8] H. van Amerongen, R. van Grondelle, Understanding the energy transfer function of LHCI, the major light-harvesting complex of green plants, J. Phys. Chem., B 105 (2001) 604–617.
- [9] C.C. Gradinaru, S. Ozdemir, D. Gulen, I.H.M. van Stokkum, R. van Grondelle, H. van Amerongen, The flow of excitation energy in LHCI monomers: implications for the structural model of the major plant antenna, Biophys. J. 75 (1998) 3064–3077.
- [10] E.I. Iseri, D. Albayrak, D. Gulen, Electronic excited states of the CP29 antenna complex of green plants: a model based on exciton calculations, J. Biol. Phys. 26 (2000) 321–339.
- [11] E.I. Iseri, D. Gulen, Chlorophyll transition dipole moment orientations and pathways for flow of excitation energy among the chlorophylls of the major plant antenna, LHCI, Eur. Biophys. J. 30 (2001) 344–353.
- [12] S. Krawczyk, Z. Krupa, W. Maksymiec, Stark spectra of chlorophylls and carotenoids in antenna pigment–proteins LHC-II and CP-II, Biochim. Biophys. Acta 1143 (1993) 273–281.
- [13] D. Olszówka, W. Maksymiec, Z. Krupa, S. Krawczyk, Spectral analysis of pigment photobleaching in photosynthetic antenna complex LHCIIb, J. Photochem. Photobiol., B Biol. 70 (2003) 21–30.

- [14] M.A. Palacios, R.N. Frese, C.C. Gradinaru, I.H.M. van Stokkum, L.L. Premvardhan, P. Horton, A.V. Ruban, R. van Grondelle, H. van Amerongen, Stark spectroscopy of the light-harvesting complex II in different oligomerisation states, *Biochim. Biophys. Acta* 1605 (2003) 83–95.
- [15] D.A. Berthold, G.T. Babcock, C.F. Yocum, A highly resolved oxygen evolving PSII preparation from spinach thylakoid membranes, *FEBS Lett.* 134 (1981) 231–234.
- [16] T.G. Dunahay, L.A. Staehelin, M. Seibert, P.D. Ogilvie, S.P. Berg, Structural, biochemical and biophysical characterization of four oxygen evolving photosystem II preparations from spinach, *Biochim. Biophys. Acta* 764 (1984) 179–193.
- [17] P. Dainese, G. Hoyer-Hansen, R. Bassi, The resolution of chlorophyll *a/b* binding proteins by a preparative method based on flat bed isoelectric focusing, *Photochem. Photobiol.* 51 (1990) 693–703.
- [18] S. Krawczyk, G. Britton, A study of protein–carotenoid interactions in the astaxanthin–protein crustacyanin by absorption and Stark spectroscopy: evidence for the presence of three spectrally distinct species, *Biochim. Biophys. Acta* 1544 (2001) 301–310.
- [19] S. Krawczyk, D. Olszówka, Spectral broadening and its effect in Stark spectra of carotenoids, *Chem. Phys.* 265 (2001) 335–347.
- [20] W. Liptay, Electrochromism and solvatochromism, *Angew. Chem., Int. Ed. Engl.* 8 (1969) 177–188.
- [21] W. Liptay, Dipole moments and polarizabilities of molecules in excited electronic states, in: C. Lim (Ed.), *Excited States*, vol. 1, Academic Press, New York and London, 1974, pp. 129–229.
- [22] D.B. Siano, D.E. Metzler, Band shapes of the electronic spectra of complex molecules, *J. Chem. Phys.* 51 (1969) 1856–1861.
- [23] G. Zucchelli, P. Dainese, R.C. Jennings, J. Breton, F.M. Garlaschi, R. Bassi, Gaussian decomposition of absorption and linear dichroism spectra of outer antenna complexes of Photosystem II, *Biochemistry* 33 (1994) 8982–8990.
- [24] D. Sandona, R. Croce, A. Pagano, M. Crimi, R. Bassi, Higher plants light harvesting proteins. Structure and function as revealed by mutation analysis of either protein or chromophore moieties, *Biochim. Biophys. Acta* 1365 (1998) 207–214.
- [25] R. Croce, R. Remelli, C. Varotto, J. Breton, R. Bassi, The neoxanthin binding site of the major light harvesting complex (LHCII) from higher plants, *FEBS Lett.* 456 (1999) 1–6.
- [26] A. Pascal, C. Gradinaru, U. Wacker, E. Peterman, F. Calkoen, K.-D. Irrgang, P. Horton, G. Renger, R. van Grondelle, B. Robert, H. van Amerongen, Spectroscopic characterization of the spinach Lhcb4 protein (CP29), a minor light-harvesting complex of photosystem II, *Eur. J. Biochem.* 262 (1999) 817–823.
- [27] A. Pagano, G. Cinque, R. Bassi, In vitro reconstitution of the recombinant photosystem II light-harvesting complex CP24 and its spectroscopic characterization, *J. Biol. Chem.* 273 (1998) 17154–17165.
- [28] R. Croce, G. Canino, F. Ros, R. Bassi, Chromophore organization in the higher-plant photosystem II antenna protein CP26, *Biochemistry* 41 (2002) 7334–7343.
- [29] R. Luchowski, S. Krawczyk, Stark spectroscopy of exciton states in the dimer of acridine orange, *Chem. Phys.* 292 (2003) 155–166.
- [30] J.M. Salverda, M. Vengris, B.P. Krueger, G.D. Scholes, A.R. Czamoleski, V. Novoderezhkin, H. van Amerongen, R. van Grondelle, Energy transfer in light-harvesting complexes LHCII and CP29 of spinach studied with three pulse echo peak shift and transient grating, *Biophys. J.* 84 (2003) 450–465.
- [31] E.J.G. Peterman, C.C. Gradinaru, F. Calkoen, J.C. Borst, R. van Grondelle, H. van Amerongen, Xanthophylls in light-harvesting complex II of higher plants: light harvesting and triplet quenching, *Biochemistry* 36 (1997) 12208–12215.
- [32] W.I. Gruszecki, W. Grudziński, A. Banaszek-Głós, M. Matuła, P. Kernen, Z. Krupa, J. Siewlewiesiuk, Xanthophyll pigments in light-harvesting complex II in monomolecular layers: localisation, energy transfer and orientation, *Biochim. Biophys. Acta* 1412 (1999) 173–183.
- [33] R. Croce, G. Cinque, A. Holzwarth, R. Bassi, The Soret absorption properties of carotenoids and chlorophylls in antenna complexes of higher plants, *Photosynth. Res.* 64 (2000) 221–231.
- [34] R. Croce, S. Weiss, R. Bassi, Carotenoid-binding sites of the major light-harvesting complex II of higher plants, *J. Biol. Chem.* 274 (1999) 29613–29623.
- [35] A. Ruban, A. Pascal, B. Robert, Xanthophylls of the major photosynthetic light-harvesting complex of plants: identification, conformation and dynamics, *FEBS Lett.* 477 (2000) 181–185.
- [36] A.V. Ruban, A. Pascal, P.J. Lee, B. Robert, P. Horton, Molecular configuration of xanthophyll cycle carotenoids in photosystem II antenna complexes, *J. Biol. Chem.* 277 (2002) 42937–42942.
- [37] S.S. Lampoura, V. Barzda, G.M. Owen, A.J. Hoff, H. van Amerongen, Aggregation of LHCII leads to a redistribution of the triplets over the central xanthophylls in LHCII, *Biochemistry* 41 (2002) 9139–9144.
- [38] V. Novoderezhkin, J.M. Salverda, H. van Amerongen, R. van Grondelle, Exciton modeling of energy-transfer dynamics in the LHCII complex of higher plants: a Redfield theory approach, *J. Phys. Chem., B* 107 (2003) 1893–1912.
- [39] J.P. Thornber, G.F. Peter, D.T. Morishige, S. Gomez, S. Anandan, B.A. Welty, A. Lee, C. Kerfeld, T. Takeuchi, S. Preiss, Light harvesting in photosystems I and II, *Biochem. Soc. Trans.* 21 (1993) 15–18.
- [40] D.S. Gottfried, J.W. Stocker, S.G. Boxer, Stark effect spectroscopy of bacteriochlorophyll in light-harvesting complexes from photosynthetic bacteria, *Biochim. Biophys. Acta* 1059 (1991) 63–75.
- [41] L.M.P. Beekman, M. Steffen, I.H.M. van Stokkum, J.D. Olsen, C.N. Hunter, S.G. Boxer, R. van Grondelle, Characterization of the light-harvesting antennas of photosynthetic purple bacteria by Stark spectroscopy: 1. LH1 antenna complex and the B820 subunit from *Rhodospirillum rubrum*, *J. Phys. Chem., B* 101 (1997) 7284–7292.
- [42] B. van Dijk, T. Nozawa, A.J. Hoff, The B800–850 complex of the purple bacterium *Chromatium tepidum*: low-temperature absorption and Stark spectra, *Spectrochim. Acta, Part A: Mol. Biomol. Spectrosc.* 54 (1998) 1269–1278.
- [43] R.N. Frese, M.A. Palacios, A. Azzizi, I.H.M. van Stokkum, J. Kruijff, M. Rogner, N.V. Karapetyan, E. Schlodder, R. van Grondelle, J.P. Dekker, Electric field effects on red chlorophylls, β -carotenes and P700 in cyanobacterial Photosystem I complexes, *Biochim. Biophys. Acta* 1554 (2002) 180–191.
- [44] T.R. Middendorf, L.T. Mazzola, K. Lao, M.A. Steffen, S.G. Boxer, Stark effect (electroabsorption) spectroscopy of photosynthetic reaction centers at 1.5 K: evidence that the special pair has a large excited-state polarizability, *Biochim. Biophys. Acta* 1143 (1993) 223–234.
- [45] T. Kakitani, B. Honig, A.R. Crofts, Theoretical studies of the electrochromic response of carotenoids in photosynthetic membranes, *Bioophys. J.* 39 (1982) 57–63.